Supporting Information for:

Explaining the formation of "triple cation" (Cs,MA,FA)Pb(Br,I)$_3$ perovskite during different stages of processing by in-situ optical monitoring

Aboma Merdasa[*a,b], Carolin Rehermann[a], Katrin Hirselandt[a], Jinzhao Li[a], Oliver Maus[a], Florian Mathies[a], Thomas Unold[c], Janardan Dagar[a], Rahim Munir[a], Eva Unger*[a,c]*

Dr. A. Merdasa, C. Rehermann, K. Hirselandt, J. Li, O. Maus, Dr. J. Dagar, Dr. R. Munir, Dr. E. Unger
Helmholtz-Zentrum Berlin für Materialen und Energie GmbH, Kekuléstraße 5, 12489 Berlin, Germany.

Dr. Thomas Unold

Helmholtz-Zentrum Berlin für Materialien und Energie GmbH, Structure and Dynamics of Energy Materials, Hahn-Meitner-Platz 1, 14109 Berlin, Germany

Dr. A. Merdasa
Department of Physics, Lund University, Sölvegatan 14, 22362, Lund, Sweden

Dr. E. Unger
Chemical Physics and NanoLund, Lund University, PO Box 118, 22100 Lund, Sweden

Keywords: perovskite, spin-coating, optical monitoring, formation kinetics,

* Corresponding Author Email: eva.unger@helmholtz-berlin.de

* Co-corresponding Author Email: aboma.merdasa@forbrf.lth.se

1) Perovskite solution preparation

To prepare precursor solutions, 1.24 M $MAPbBr_3$ (0.087 g $PbBr_2$ with 0.0225 g MABr were dissolved in a 4:1 volume ratio of 0.13 ml DMF and 0.032 ml DMSO), 1.24 M $FAPbI_3$ (0.5435 g PbI_2 with 0.1682 g FAI were dissolved in 0.630 ml DMF and 0.157 ml DMSO), then they were mixed in a 83:17 volume ratio($(FAPbI_3)_{0.83}$ $(MAPbBr_3)_{0.17}$). Finally, nominal 1.5 M CsI (0.0195 g CsI dissolved in 0.05 ml DMSO) was added into $(FAPbI_3)_{0.83}$ $(MAPbBr_3)_{0.17}$ in a 5:95 volume ratio.

2) Solar cell preparation & characterization

p-i-n devices

Patterned ITO substrates were cleaned with soap water, DI water, acetone, and propanol for 15 minutes each followed by 15 minutes of UV-ozone treatment. PTAA (2mg/ml) in Toluene is spin coated (4000 rpm for 35 seconds) on the cleaned ITO coated substrates and annealed at 100 oC for 10 minutes. Then, perovskite solution is spin coated (4000 rpm for 40 seconds) on PTAA coated substrates. Ethyl acetate is dripped at 25 seconds of spin coating time as anti-solvent followed by annealing at 100 ^{o}C for 1 hour. C60 (23 nm), BCP (8 nm), and Cu (100 nm) is thermally evaporated on the perovskite coated substrates.

n-i-p devices

Patterned ITO substrates were cleaned with soap water, DI water, acetone, and propanol for 15 minutes each followed by 15 minutes of UV-ozone treatment. The $SnCl_2.2H_2O$ solution (0.1M in ethanol) is spin coated on ITO in two steps 1500 rpm and 2500 rpm for 30 seconds each. Films were

annealed at 170 °C for one hour in air and afterwards they were subjected to UV-O_3 treatment for 25 minutes. The perovskite deposition is same as mentioned for p-i-n devices however, chlorobenzene is used as anti-solvent. Spiro-OMeTAD precursor with 36.2 mg/mL in chlorobenzene and TBP (14.4µL/mL), LiTFSI (8.8µL/mL), and cobalt(III) complex (14.5µL/mL) was deposited on the perovskite film by spin coating at 1800 rpm for 30 seconds. 80 nm of Au gold is thermally evaporated.

Device characterization

Current density-Voltage (J-V) measurements of p-i-n devices were measured in nitrogen purged glove box using a Wavelabs Sinus-70 sun simulator with AM 1.5G spectra at an intensity of 1000 W/m^2 (1 sun) calibrated with silicon solar cell (Fraunhofer ISE). The voltage step, delay time, and integration time for data point scans were fixed at 20 mV, 40 ms, and 20 ms respectively for each cell measurements in both forward and reverse scan. The n-i-p devices were measured in ambient environment with the same parameters as p-i-n devices. The active area in both the devices is 0.16 cm^2. Figure S1 shows device performance for both regular and inverted solar cells employing the described recipes.

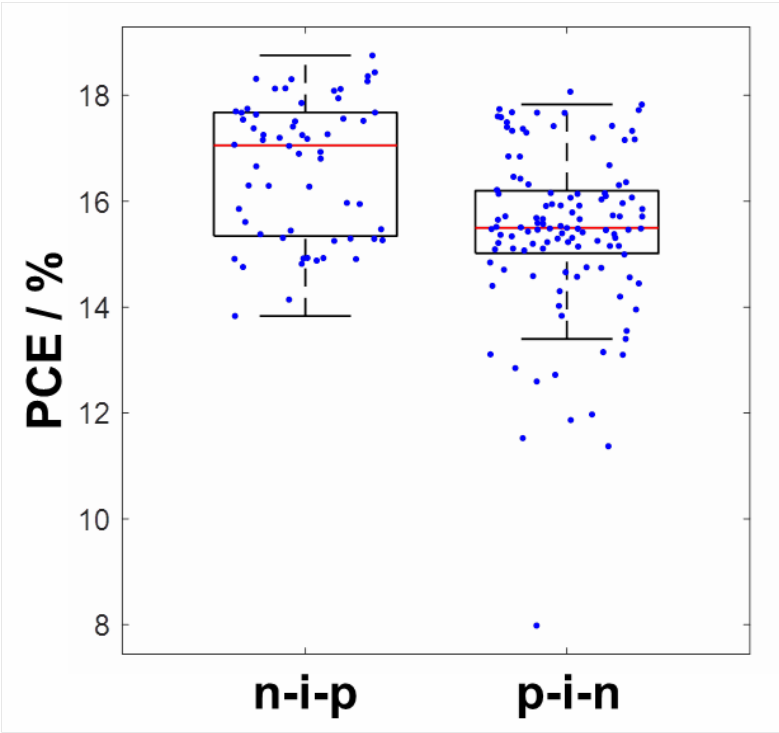

Figure S1. Device performance statistics of regular and inverted devices.

3) Thickness validation

Bisphenol A ethoxylate diacrylate has a spectrally averaged refractive index of 1.54 +/- 0.079 between 450 – 850 nm. The material was spin-coated onto a silica wafer and its thickness was measured with a Bruker dektak profilometer and determined to have a thickness of 1040 nm. We then determined the thickness in the optical monitoring setup. Figure S2a shows the interference pattern of the film on the rotating spin-coater measured for 10 seconds. The pattern does not change with time, which of course makes sense since the thickness is not changing. Therefore, we can rule that any changes in the interference pattern during thinning is caused by the experimental setup itself. Figure S2b shows the time averaged interference pattern converted into units of wavenumbers. The red trace represents the refractive index calculated using the Cauchy formula. For the calculation we use an average refractive index (<n>) of 1.54 since the variance over the spectral range is not significant to produce large fluctuations of the thickness. The thickness extracted using Equation (2) in the main text is 1062 nm +/- 24 nm, which is in excellent agreement with the thickness determined using the profilometer.

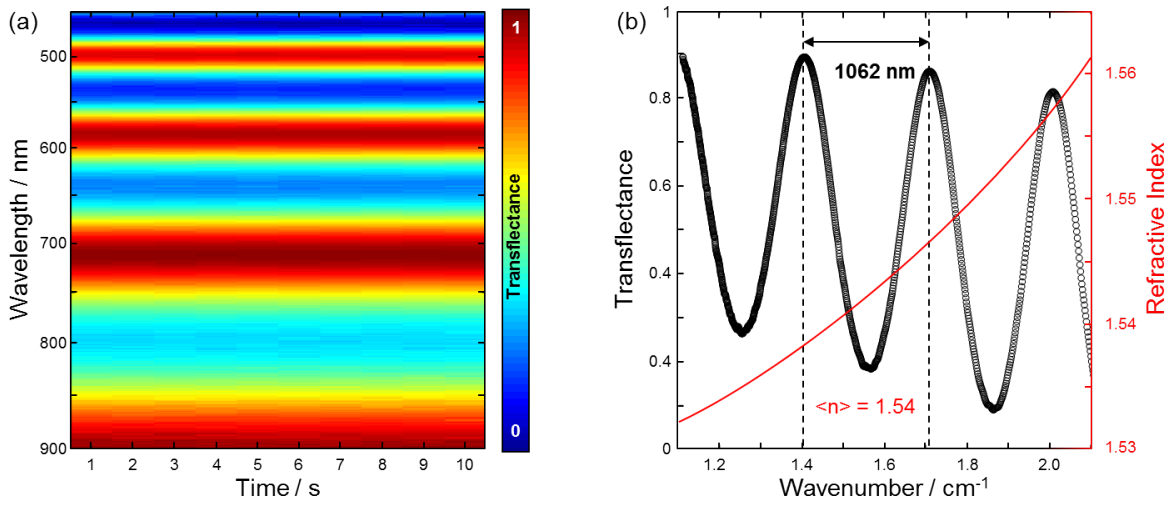

Figure S2. (a) interference pattern of the photo resist film on Si-wafer measured for 10 seconds on the rotating spin-coater (4000 rpm). (b) Time averaged interference pattern converted into units of wavenumbers (black circles) together with the energy dependent refractive index (red line) in the same spectral range as the interference pattern.

4) Interference measurements on substrates with Ag-mirror

During spin-coating, we can observe a number of different processes and should consider how to optimize the experimental conditions to maximize each. If it is of interest to capture the thinning, granted that the absolute thickness is more than 300-400 nm (depending on precursor refractive index).

The thickness is extracted from the interference pattern that arises due to the incoming light partially reflecting back from the top surface of the relatively smooth film, and then surface that is on the opposite side of the film. The visibility of the interference pattern will depend on the relative signal strength of the two reflections. If i.e. the top does not reflect much light (due to a rough surface) or if the bottom surface does not reflect much light (due to high transmission), an interference pattern will be either very weak or not detected. This is why we spin coat a layer of silver on top of the substrate to increase the reflectivity. Note, that this may alter crystallization processes of the film, which may be circumvented by spin-coating a thin buffer or transport layer. In this scenario (let's call it 'AG-up'), absorption can also be observed, however, if the relative intensity of the light manages to penetrate the now absorbing film and reflect back off of the AG layer is comparable to the light that reflects off the top (assuming still relatively smooth) film surface, an interference can still be observed. In this scenario, the absorption onset and interference pattern will be mixed giving rise to something shown in Figure 1a. A problem with this is that the actual absorption onset may be obscured by the interference pattern.

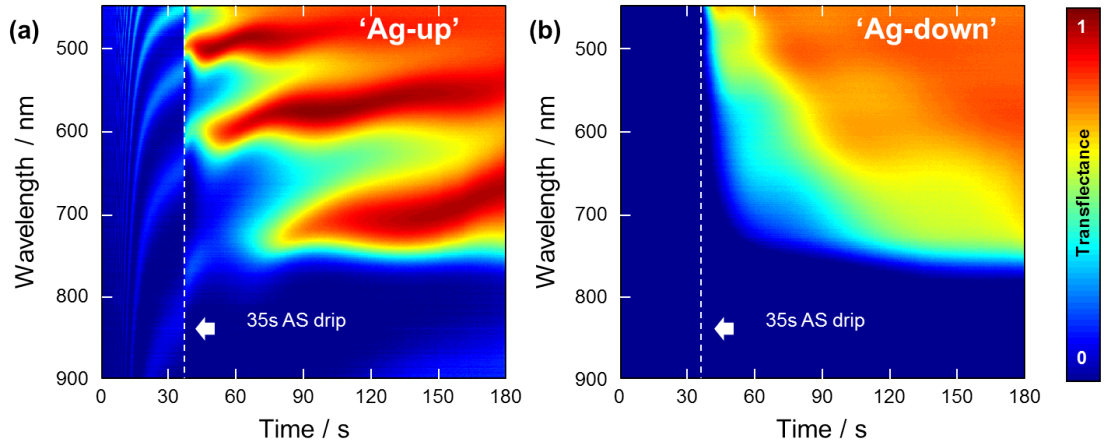

Figure S3. Heat maps of transflectance measured with (a) Ag surface facing up and (b) Ag surface facing down.

Due to this issue, one should instead place the silver coated surface such that it faces the spin-coater if one wants to get a more reliable absorption signal and absorption onset (let's call this scenario 'Ag-down'). This is demonstrated in Figure 1b which is a repeated measurement of that shown in Figure 1a only changing the orientation of the Ag-coated substrate. The reason why an interference pattern is not seen here is because most of the light striking the substrate after passing the film will transmit and then get reflected from the silver now facing the spin-coater. This should in principle also yield a combination of interference patterns, one very weak from the thinning film, and another weak from the constant substrate. If we were able to detect these based on signal strength, we would still not be able to see the interference pattern from the substrate since its thickness would yield fringes of high frequency. As shown in Figure 1b, we do not observe fringes.

While it is important to decide prior to measuring which direction the silver should face, this feature could be taken advantage of by measuring on both sides in two consecutive measurements as shown in Figure 1. Under the assumption that the pattern observed in Figure 1a is simply a linear combination of the signals (interference and absorption), we could in principle subtract the signal generated in the 'Ag-down' scenario from the 'Ag-up scenario'. This is shown in Figure 2a where we can almost see a continuation of the interference pattern prior to applying the AS drip (indicated with black dashed lines). There is some variation, and that is most likely caused by the properties of the crystallizing film changing

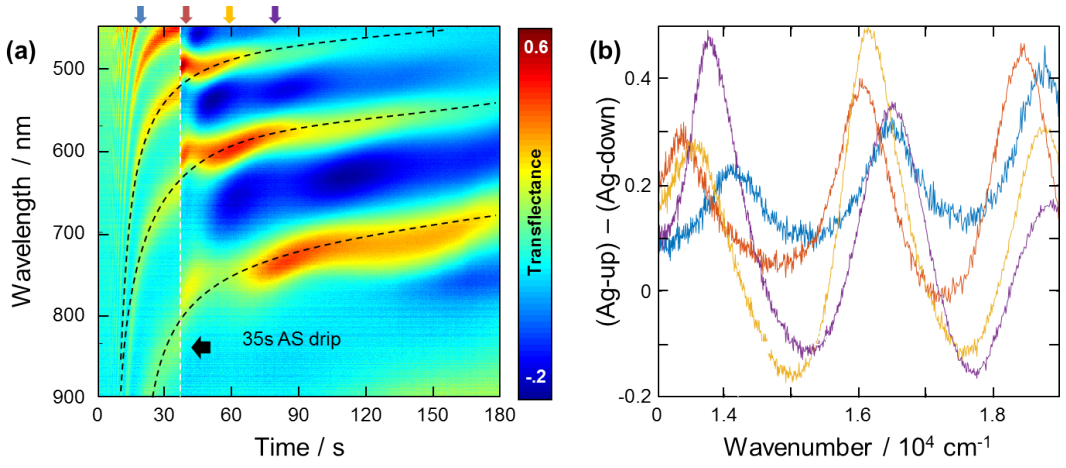

Figure S4. (a) Heat map showing the difference of transflectance measured with Ag-surface facing up and down. (b) selected transflectance spectra from the four times indicated with the colored arrows in (a).

If we look at the interference pattern at a couple of selected points indicated with the colored arrows above Figure 2a, we can see clear interference patterns where thicknesses could be extracted (Figure 2b). Assuming that the thickness doesn't change too much when applying the AS drip, one could

potentially attribute the changing 'thickness' extracted from the separating fringes to a changing refractive index.

However, if we finally get to the issue of whether the absorption onset can be trusted in the case when there is an interference pattern, Figure 3 shows a comparison between the last spectrum extracted from the two heat maps in Figure 1 as well as the one from Figure 2a.

In this case we can see that there is a very small change in the absorption onset, but this is due to the large fringe aligning quite well with the onset in order to minimally perturb it. My gut feeling tells me there is a physical reason for this, but I don't know it. Neither can I say if it always ends up being like this from one measurement to another of the same compound or if it is consistently different for another compound.

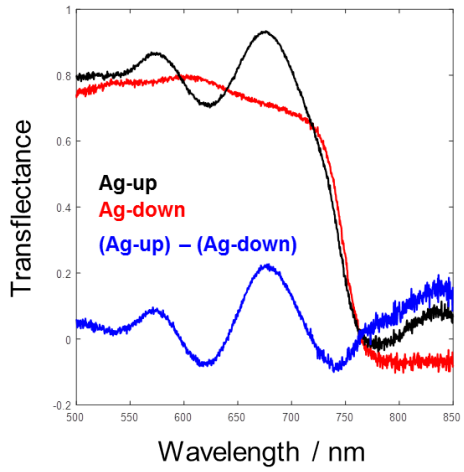

Figure S5. Comparison of absorption spectra with Ag-side up, down and the difference between spectra.

5) Rheology Measurements

Dynamic viscosity was measured with an Automated Micro Viscometer (AMVn) from Anton Paar. A cleaned capillary (Ø = 1.6 mm) was filled under ambient conditions with a stainless steel ball (ρ = 7.62 g/cm³; Ø = 1.5 mm) and the sample solution. The capillary was set to an angle of 70° with respect to the horizon and each measurement was carried out with four repetitions at 20 °C. Refractive index was measured with an Abbé refractometer from Krüss. The refractive index as well as density

vary linearly with solution concentration while the dynamic viscosity increases more exponentially with higher solution concentrations.

Table S1. Summary of solution viscosity $\boldsymbol{\eta}$ determined from derivation of K as function of time (EBP model) as well as extrapolation from Meyerhofer plots for different spin coating speeds

Spin coating speed rpm	**Viscosity η EBP / from initial K[cP]**	**Viscosity η Meyerhofer [cP]**	**Viscosity η Rolling ball viscometer [cP]**	**Evaporation parameter E [μm s^{-1}]**
2000	8.16	8.25	-	0.111
3000	10.0	7.78	-	0.128
4000	8.41	7.85	-	0.153
5000	8.34	9.55	-	0.148
6000	9.01	9.29	-	0.131
average	8.78 ± 0.75	8.54 ± 0.82	8.43 ± 0.31	

Table S2. Summary of solution viscosity $\boldsymbol{\eta}$ determined from derivation of K as function of time (EBP model) as well as extrapolation from Meyerhofer plots for different precursor concentrations.

Precursor concentration [M]	**Viscosity η EBP / from initial K[cP]**	**Viscosity η Meyerhofer [cP]**	**Viscosity η Rolling ball viscometer [cP]**	**Evaporation parameter E [μm s^{-1}]**
0.8	3.49	1.57	3.52	0.07
1.0	4.83	2.94	5.07	0.11
1.2	8.29	6.18	8.43	0.18

PL evolution on different substrates

The temporal evolution of the PL signal as shown in Figure 4b was repeated for perovskite crystallization on both PTAA and PEDOT:PSS (Figure S3), which are both relevant transport layers for many perovskite based solar cells. The peculiar trend of the relative PL intensity is repeatable which therefore rather reflects a material property than an experimental artifact.

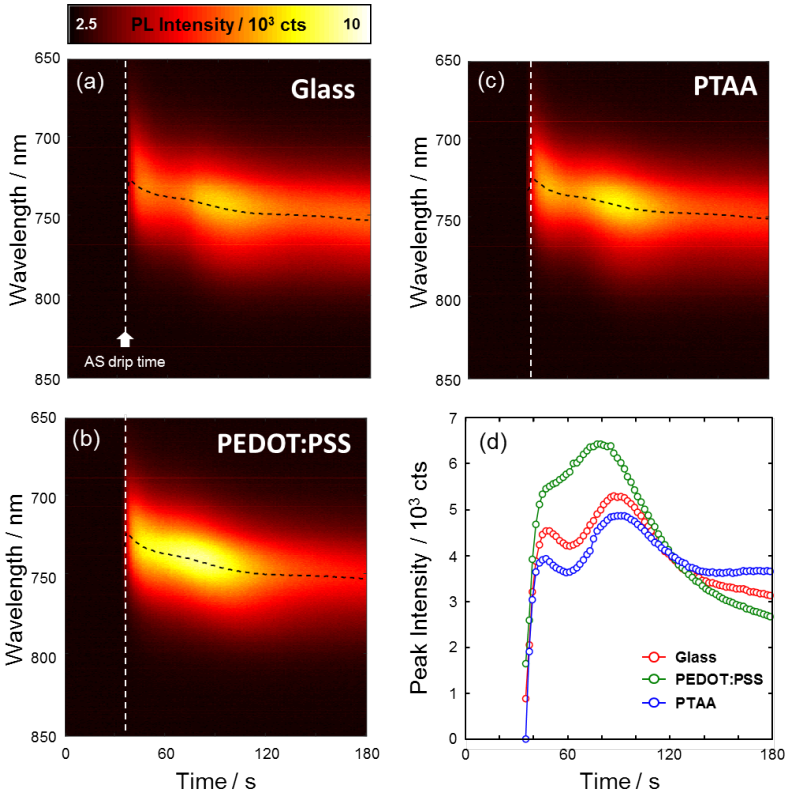

Figure S3. 2D heat maps showing the spectral evolution of the PL signal of the AS-drip induced perovskite crystallization on (a) glass, (b), Pedot:PSS, and (c) PTAA. (d) PL intensity evolution of the PL spectral peak.

Filename: Merdasa_3CATformation_SI_JMCA2020.docx
Folder: /Users/evlithun/Documents/PUBLICATIONS/2020_06_InSituSetup_Merdasa/2020_03_TechnicalPaper_Merdasa/JMCAsubmission
Template: /Users/evlithun/Library/Group Containers/UBF8T346G9.Office/User Content.localized/Templates.localized/Normal.dotm
Title:
Subject:
Author: Munir, Rahim
Keywords:
Comments:
Creation Date: 24/05/2020 20:40:00
Change Number: 3
Last Saved On: 04/08/2020 21:57:00
Last Saved By: Eva Unger
Total Editing Time: 7 Minutes
Last Printed On: 03/11/2020 21:54:00
As of Last Complete Printing
Number of Pages: 9
Number of Words: 1.889 (approx.)
Number of Characters: 10.772 (approx.)